1459

Ecological Modelling, 67 (1993) 179–198
Elsevier Science Publishers B.V., Amsterdam

An empirical model for predicting diurnal air-temperature gradients from edge into old-growth Douglas-fir forest

Jiquan Chen [a], Jerry F. Franklin [a] and Thomas A. Spies [b]

[a] *College of Forest Resources, University of Washington, Seattle, WA, USA*
[b] *Forestry Sciences Laboratory, USDA Forest Service, Pacific Northwest Research Station, Corvallis, OR, USA*

(Received 3 January 1992; accepted 9 July 1992)

ABSTRACT

Chen, J., Franklin, J.F. and Spies, T.A., 1993. An empirical model for predicting diurnal air-temperature gradients from edge into old-growth Douglas-fir forest. *Ecol. Modelling*, 67: 179–198.

Edge — the boundary line between clearcut and adjacent old-growth forest — is one of the critical landscape elements in the highly fragmented forest landscapes of North America's Pacific Northwest. Ecological phenomena at edges may be better understood by examining the physical environments near the edge. To further this objective diurnal air temperature gradients were measured along 16 gradients from the edge into the interior old-growth Douglas-fir [*Pseudotsuga menziesii* (Mirb.) Franco] forest over the 1989 and 1990 growing seasons and analyzed effects of edge orientation (relation of edge-facing to the azimuth) and macroclimate (local weather conditions of the clearcut) on these gradients were also explored through regression analysis. The air temperature gradient was expressed with a simple exponential equation involving three intermediate variables of interest: air temperature in the interior forest (*TEMPIF*), difference in air temperature between the edge and inside the forest (ΔAT), and changing ratio of temperature along the gradient (*SLOPE*). Linear or nonlinear regression equations were developed to predict *TEMPIF*, ΔAT, and *SLOPE*. Correlation analysis always preceded regression analysis, in which the relationships between the regression parameters and independent variables representing edge orientation and macroclimate were further explored. A computer model developed from the final empirical relationships successfully predicted air temperature gradients, circumventing the need for time-consuming field measurements with expensive meteorological instruments, and generated new information about the influences of edge orientation and macroclimate on air temperatures. *TEMPIF*, ΔAT, and *SLOPE* were shown to be highly sensitive to the dependent variables. Although model application should be limited to

Correspondence to: Jiquan Chen, College of Forest Resources, University of Washington, Seattle, WA 98195, USA.

edges created by recent (10- to 15-year-old) clearcuts adjoining old-growth Douglas-fir forest, the modeling approach could be applied to edges with different characteristics by modifying the relationships.

INTRODUCTION

Extensive use of dispersed clearcutting in the last several decades has created a highly fragmented ("checkerboard") forest landscape in North America's Pacific Northwest (Franklin and Forman, 1987). As a result, edge — the boundary line between clearcut and adjacent old-growth forest — has become one of the most important features of this landscape. Indeed, forest values such as wildlife habitat and biological diversity have been fundamentally changed because of the significant amount of edge and result *edge effects* created by the "checkerboard" (Yahner, 1988; Franklin, 1989; Lehmkuhl and Ruggiero, 1991).

Environment of the edge is unique, clearly distinguishable from that of the clearcut and interior forest (Chen, 1991). Both biological (Chen et al., 1992) and physical variables respond to edge environments, producing edge effects (i.e., ecological phenomena associated with edge). For instance, as one moves along a gradient from the edge into the old-growth Douglas-fir [*Pseudotsuga menziesii* (Mirb.) Franco] forest, the microclimate changes considerably depending on edge orientation (i.e., relationship of edge-facing to the azimuth) and macroclimate (i.e., local weather conditions). Air temperature — one of the key variables characterizing energy flow in the biosphere (Lee, 1978; Campbell, 1986) and critical to predicting other meteorological variables (Bocock et al., 1977; Taconet et al., 1986; Dwyer et al., 1990), ecosystem processes in the Douglas-fir forest (Zobel et al., 1976; Waring and Franklin, 1979; Chapin et al., 1987), and natural disturbances (Beck and Trevitt, 1989) — is of particular interest.

The ability to predict microclimatic patterns near forest edges under specific macroclimatic conditions across a range of edge orientations is important to those managing forest resources. To this end, we (1) examine the empirical relationships between air temperature, edge orientation, and macroclimate along gradients from the edge into the old-growth Douglas-fir forest, (2) use regression analysis to develop a computer model based on those empirical relationships to predict diurnal air temperatures over such gradients during the growing season, and then (3) evaluate the model's ability to predict gradients for varying edge orientations and macroclimates. Our results can be used as inputs to ecological simulation models (e.g., Dale and Hemstrom, 1984; Running et al., 1989) and as an independent variable for analyzing biological processes (e.g. Edmonds, 1987; Peters, 1990; Dreistadt et al., 1991).

STUDY AREA AND DATA COLLECTION

The two study areas are located on the western slope of the Cascade Range: the Wind River Experimental Forest, 45°48′ N and 121°55′ W, on the Gifford Pinchot National Forest in southern Washington; and the H.J. Andrews Experimental Forest, 44°14′ N and 122°11′ W on the Willamette National Forest in central Oregon. Elevation of the study areas ranges from 650 to 1000 m; slopes are gentle (< 10°). The forests are representative of typical old-growth Douglas-fir forest in western Oregon and Washington and occupy typical sites of the *Tsuga heterophylla* and lower *Abies amabilis* Zones (Franklin and Dyrness, 1973). Major tree species include Douglas-fir, western hemlock [*Tsuga heterophylla* (Raf.) Sarg.], Pacific silver fir (*Abies amabilis* Dougl. ex Forbes), Pacific yew (*Taxus brevifolia* Nutt.), and western redcedar (*Thuja plicata* Donn ex D. Don) (Franklin et al., 1981). Dominant trees are typically 50–60 m tall.

We selected for study 16 edges (13 at Wind River, 3 at H.J. Andrews) along old-growth forest patches created when adjacent forest was clearcut 10–15 years earlier. The forest patches are more than 500 m in diameter so as to provide an interior forest environment at least near their center. The clearcuts were subsequently planted with several conifer species; regenerating trees on these cutover areas were generally less than 2.5 m tall.

At each of the 16 sites, we randomly located a transect extending from each edge (0 m) into interior (240 m from the edge) old-growth forest and established six sampling stations (0, 30, 60, 120, 180, and 240 m from the edge) along it. The seventh sampling station, the center of the clearcut — determined from aerial photos and ground measurements — provided the macroclimatic data. All edges were coded and their orientations (0–360°; 0 = north, 90 = east, 180 = south, 270 = west) recorded. At each sampling station over two growing seasons (late June through September, 1989 and 1990), air temperature was measured every 15 s with thermocouples and Campbell's 21X microloggers 2 m above the ground; measurements were averaged over 30-min intervals. Equipment remained at each transect until a clear day was recorded (usually 3–10 days), then was moved to another transect.

MODEL DEVELOPMENT

Modeling basics

The air temperature gradient into the forest for any given time t (0–24 h) can be expressed by a simple exponential equation:

$$TEMP(t) = TEMPIF(t) + \Delta AT(t)\exp[-SLOPE(t) * \delta] \qquad SLOPE(t) \geq 0 \tag{1}$$

where *TEMP* is air temperature (°C) at time t and δ is distance (m) from the edge into the forest. *TEMPIF*, ΔAT, and *SLOPE* are the primary intermediate variables of interest herein, representing, respectively, air temperature in the interior forest, difference in air temperature between the edge and forest, and change ratio of temperatures along the gradient. A positive ΔAT indicates that air temperatures decrease with distance from the edge, a negative ΔAT that they increase. Diurnal changes in air temperature from the edge into the forest can be predicted by simulating the dynamics of these three variables over a 24-h period.

TEMPIF, ΔAT, and *SLOPE* were independently estimated from field data (134 days of air temperatures) through regression analysis. First, appropriate regression equations were fit to the data for each of the three variables of interest. We further examined the relationships between these parameters involved and five independent variables representing edge orientation (θ) and macroclimate through correlation analysis and then developed further regression equations, generating final equations for the relationships between *TEMPIF*, ΔAT, and *SLOPE* and edge orientation and macroclimate:

$$TEMPIF = \text{function } (T_{\min}, T_{\max}, T_{\min 2})$$

$$\Delta AT = \text{function } (\theta, T_{\max 1}, T_{\min}, T_{\max}, T_{\min 2})$$

$$SLOPE = \text{function } (\theta, T_{\min}, T_{\max}, T_{\min 2})$$

Four independent variables used to describe the macroclimate are: $T_{\max}$ (daily maximum), $T_{\min}$ (daily minimum), $T_{\max 1}$ (the previous day's maximum), $T_{\min 2}$ (the next day's minimum air temperature). Based on these relationships, a computer model written in TURBO C^{++} was developed to predict diurnal air-temperature gradients with distance from the edge into interior forest given specific information on edge orientation and macroclimatic conditions. Edge effects were evaluated via combinations of ΔAT and *SLOPE*, which are highly correlated because of their intrinsic relationship in equation (1), the basis for model development. The model was verified by examining the sensitivities of *TEMPIF*, ΔAT, and *SLOPE* to edge orientation and macroclimate.

Following is a detailed explanation of how we estimated each of the three intermediate variables composing the empirical model for predicting diurnal air-temperature gradients.

Estimation of TEMPIF

The literature proposes many methods for simulating the diurnal pattern of air temperatures based on energy budget (Myrup, 1969; Lemon et al., 1971; Miller, 1980) or empirical data (Parton and Logan, 1981). Empirical equations include simple curve fitting based on sine and exponential curves (Allen, 1976; DeWit et al., 1978; Parton and Logan, 1981; Acock et al., 1983; Floyd and Braddock, 1984) or sophisticated Fourier analysis (Carson, 1963; Walter, 1967; Watanabe, 1978). We chose simple curve fitting, which is more widely used and recommended than Fourier analysis (Wann et al., 1985; Rothermel et al., 1986; Beck and Trevitt, 1989; Hungerford et al., 1989; Reicosky et al., 1989).

We used a simple combination of sinusoidal curve fitting in this study. A similar method, previously applied (DeWit et al., 1978; Floyd and Braddock, 1984; Hoogenboom and Huck, 1986; Rothermel et al., 1986), was found to be the best under most circumstances (Reicosky et al., 1989). The original approach requires the daily maximum and minimum temperatures and the times of these extremes. We modified that approach in three ways: (1) by adding to the simulation T_{max1} and T_{min2} which provide the information on trends in local weather condition, (2) by empirically estimating the time of the temperature extremes t_1 (time of minimum temperature) and t_2 (time of maximum temperature), and (3) by beginning the simulation period at one t_1 and ending it at the next t_1. In fact, the simulation period was divided into two segments: (1) t_1 to t_2, and (2) t_2 to the next t_1. Traditionally, t_1 and t_2 have been calculated from time of sunrise and sunset depending upon the location (latitude and longitude) of study sites and days of the year (DeWit et al., 1978; Parton and Logan, 1981; Beck and Trevitt, 1989). However, in our study, these two variables did not significantly correlate with location and Julian day (by a F-test) so that the means were used. The means computed for t_1 ($n = 114$) and t_2 ($n = 119$) from the field data for the two seasons studied were 5.43 and 14.40 h, respectively. The model algorithms are:

$$TEMPIF = \begin{cases} T_{av1} - \mathrm{AMP}_1\{\cos[\pi(t - t_1)T']\} & t \le t_2 \\ T_{av2} - \mathrm{AMP}_2\{\cos[\pi(t + L')/(24 - T')]\} & t > t_2 \end{cases} \qquad (2)$$

where

$T_{av1} = (T_{min} + T_{max})/2$

$\mathrm{AMP}_1 = (T_{min} - T_{max})/2$

$T_{av2} = (T_{min2} + T_{max})/2$

$\mathrm{AMP}_2 = (T_{max} - T_{min2})/2$

$T' = t_2 - t_1$

$L' = (24 - T') - t_2$

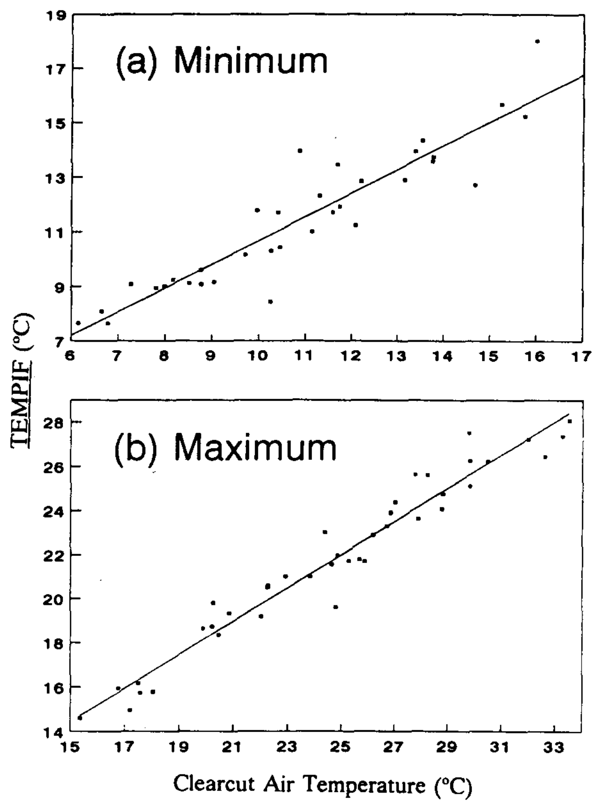

Fig. 1. Linear relationship of diurnal air temperature in the interior forest (*TEMPIF*) and local macroclimate (i.e. air temperature of adjacent clearcut); $n = 34$ (minimum temperatures) and 39 (maximum temperatures).

T_{max} and T_{min} were found to be linearly related to the corresponding maximum and minimum temperatures in the clearcut (T_{maxc} and T_{minc}, respectively) by the following simple linear regression equations (Fig. 1):

$$T_{max} = 3.1012 + 0.7556\ T_{maxc} \quad R^2 = 0.95 \text{ and MSE} = 0.736$$

$$T_{min} = 2.1859 + 0.8566\ T_{minc} \quad R^2 = 0.84 \text{ and MSE} = 1.034$$

Estimation of ΔAT

As for *TEMPIF*, the diurnal pattern of ΔAT values also produces a sinusoidal curve (Fig. 2). Two-stage regression analysis was used to estimate ΔAT. In first-stage regression, we divided the curve in two, before

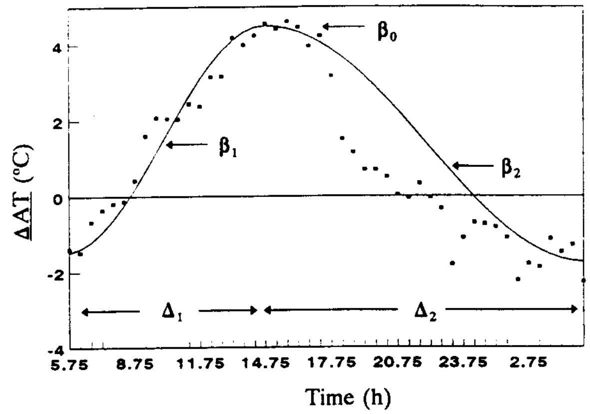

Fig. 2. Difference in diurnal air temperature between edge and interior forest (ΔAT), and β_0 is the maximum ΔAT, β_1 is the average air temperature during time interval Δ_1, and β_2 is the average temperature during time interval Δ_2.

and after time of maximum ΔAT (t'), and fit this curve with the following equations:

$$\Delta AT = \begin{cases} \beta_0 - (\beta_0 - \beta_1)\cos(\pi t/\Delta_1) & t \le t' \\ \beta_2 - (\beta_0 - \beta_2)\cos[\pi(t+\Delta)/\Delta_2] & t > t' \end{cases} \tag{3}$$

where β_0 is the maximum ΔAT, β_1 is the average ΔAT during time interval Δ_1 (calculated as t'–5.43, where 5.43 is the estimated mean for T_1), β_2 is the ΔAT during time interval Δ_2 (calculated as 24–Δ_1), and Δ is the difference between Δ_1 and Δ_2 (Δ_2–Δ_1).

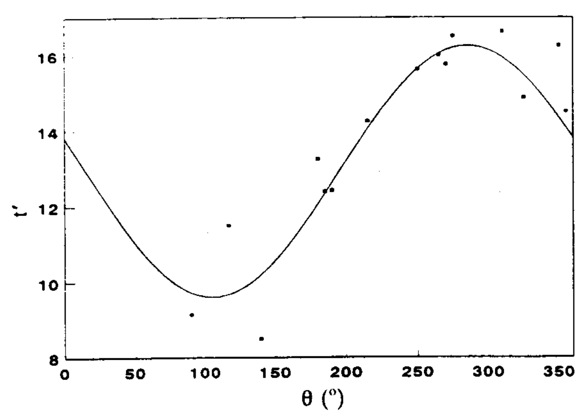

Fig. 3. Timing of the maximum ΔAT (t') as a function of edge orientation (θ); t' occurs earliest at an northeast-facing edge ($\theta = 74.8$) and latest at a southwest-facing edge ($\theta = 254.8$).

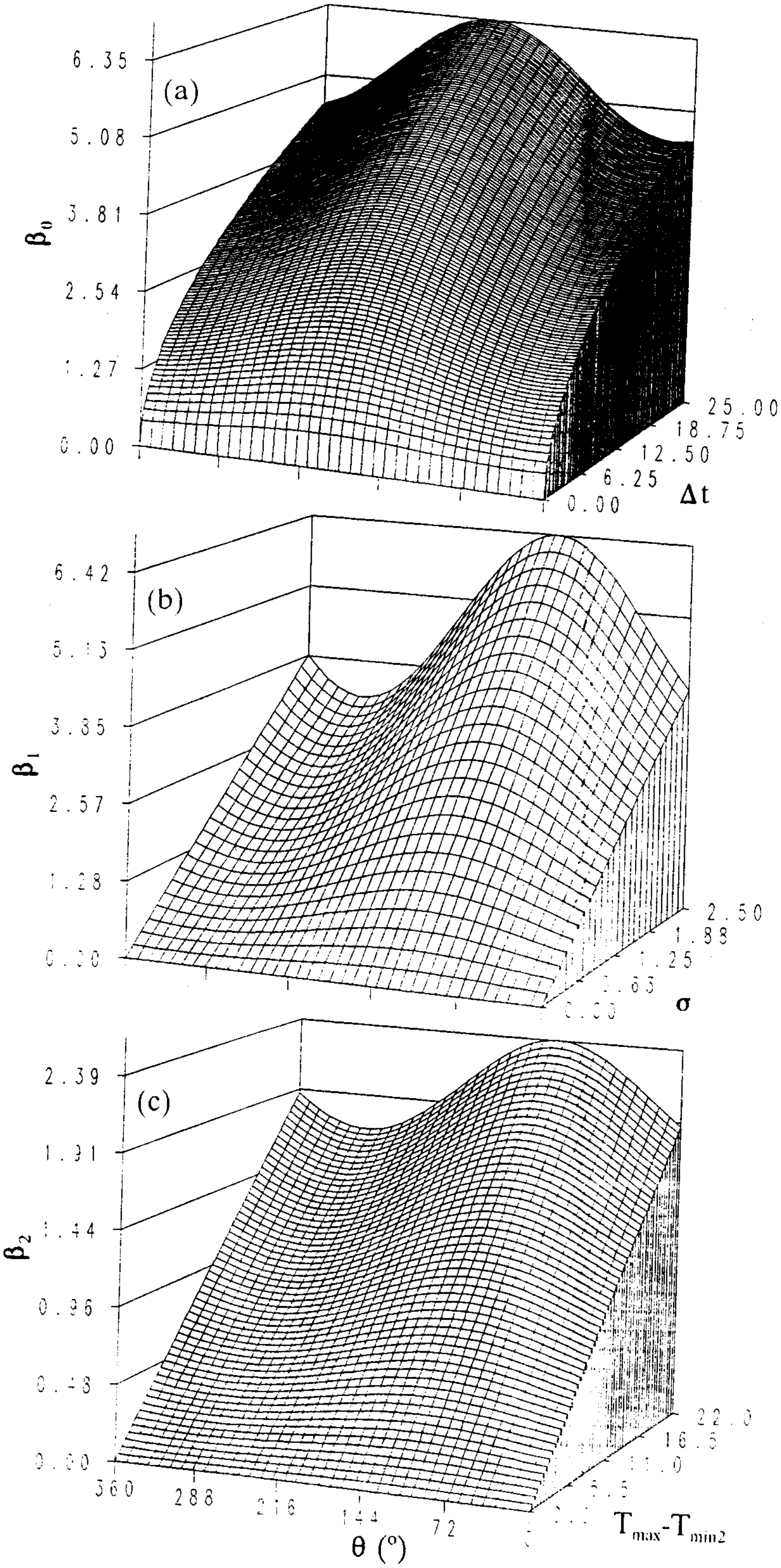
(a)
β_0
6.35
5.08
3.81
2.54
0.00
25.00
18.75
12.50
6.25
0.00
Δt
(b)
β_1
6.42
3.85
2.57
2.50
1.88
1.25
σ
(c)
β_2
2.39
0.96
0.00
22.0
16.5
360
288
216
144
72
θ (°)
T_{max}-T_{min2}

Correlation analysis showed that t' was strongly related to θ (Fig. 3). Thus, in second-stage regression, we fit the following cosine equation (non-linear) to estimate t':

$$t' = 12.925 + 3.3216 \cos[\pi(\theta + 74.78)/180] \quad \text{MSE} = 2.793$$

In this equation, the value 74.78 indicates that maximum ΔAT occurs earliest at a northeast-facing edge.

Correlation analysis showed that β_0 was strongly related to θ and diurnal temperature fluctuation, Δt (i.e., T_{max}–T_{min}). In second-stage regression, we square-root transformed the independent variables (Δt) and fit the following non-linear equation to estimate β_0:

$$\beta_0 = \text{sqrt}(\Delta t)\{1.0869 + 0.1828 \cos[\pi(\theta - 197.18)/180]\} \quad \text{MSE} = 1.372$$

In this equation, the value 197.18 indicates that β_0 is maximum at a southwest facing edge (Fig. 4a).

Correlation analysis showed that β_1 appeared to be highly related to T_{max}, T_{min}, T_{max1}, θ, and a new variable, σ [i.e., $(T_{max}–T_{min})/(T_{max1} - T_{min})$], representing the ratio of diurnal temperature fluctuation. β_1 values were larger near southeast-facing edges with higher values of σ. Therefore, we fit the following non-linear equation in second-stage regression to estimate β_1:

$$\beta_1 = \sigma\{1.9230 + 0.6459 \cos[\pi(\theta - 126.09)/180]\} \quad \text{MSE} = 0.649$$

In this equation, the value 126.09 indicates that β_1 is maximum at a southeast-facing edge regardless of changes in σ. The predicted pattern is illustrated in Fig. 4b.

Correlation analysis showed that β_2 was significantly related to θ and diurnal temperature difference between T_{max} and T_{min2}. In second-stage regression, we fit the following non-linear equation to estimate β_2:

$$\beta_2 = (T_{max} - T_{min2})\{0.0927 + 0.01612 \cos[\pi(\theta - 115.26)/180]\}$$
$$\text{MSE} = 0.686$$

In this equation, the value 115.26 indicates that β_2 is maximum at a southeast-facing edge. The predicted pattern is illustrated in Fig. 4c.

Fig. 4. Distributions, from second-stage regression, of predicted (a) β_0 values relative to edge orientation (θ) and diurnal temperature fluctuation, Δt (i.e. $T_{max}-T_{min}$), (b) β_1 values relative to θ and the ratio of diurnal temperature fluctuation, σ [i.e., $(T_{max}-T_{min})/(T_{max1}-T_{min})$], and (c) β_2 values relative to θ and diurnal temperature fluctuation, σ (i.e. $T_{max}-T_{min2}$). T_{max} and T_{min} = daily maximum and minimum air temperatures, respectively; T_{max1} = previous day's maximum; T_{min2} = next day's minimum.

Estimation of SLOPE

SLOPE was estimated from field data for *TEMPIF* and ΔAT to void the autocorrelation between *SLOPE* and the other two variables. Two-stage regression analysis was used again to estimate *SLOPE*. Prior analysis (correlation analysis) suggests that changes in *SLOPE* over time are related to macroclimate. Because $T_{max}-T_{min}$ plays an important role in determining *SLOPE* before 14.40 h (the computed mean for t_2) and $T_{max}-T_{min2}$ after 14.40 h, in first-stage regression we divided the sinusoidal curve in two sections and fit the data with the following equation (nonlinear):

$$SLOPE = \gamma\{\kappa_0 + \kappa_1 \cos[\pi(\theta - \kappa_2)/180]\} \tag{4}$$

where κ_0, κ_1, and κ_2 were the parameters need further estimation in second-stage regression. γ is the variable computed as follows:

$$\gamma = \begin{matrix} T_{max}-T_{min} & t \leq 14.40 \\ T_{max}-T_{min2} & t > 14.40 \end{matrix}$$

SLOPE estimates had to be corrected after first-stage regression. A very large (> 0.5) or small (< 0.004) *SLOPE* value suggests the absence of a clear edge effect (Fig. 5). Hence, before further statistical analysis, estimated *SLOPE* values were reset to zero if they fell outside the range 0.004–0.5 (i.e., if there was no edge effect).

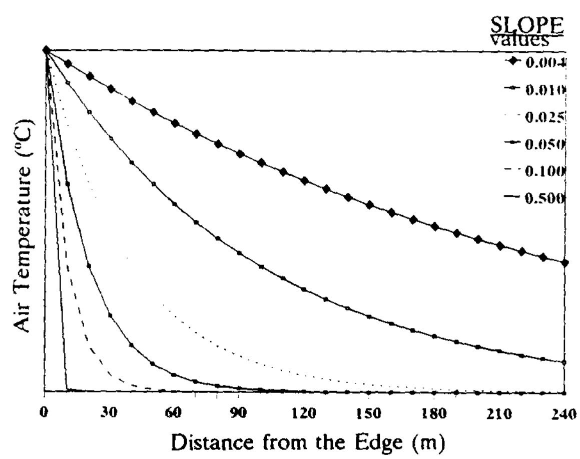

Fig. 5. Effect of changing ratio of diurnal air temperatures from edge into interior forest (*SLOPE*) on temperature in the interior forest (*TEMPIF*) with distance from the edge. *SLOPE* values > 0.05 (fast change over short distance) or < 0.004 (little or no change over long distance) are not considered in the model because they do not produce meaningful edge effects.

'PIF and ΔAT to void
wo variables. Two-stage
SLOPE. Prior analysis
E over time are related
ant role in determining
) and T_{max}–T_{min2} after
inusoidal curve in two
ı (nonlinear):

(4)

further estimation in
as follows:

age regression. A very
ests the absence of a
atistical analysis, esti-
ell outside the range

:dge into interior forest
listance from the edge.
little or no change over
ıot produce meaningful

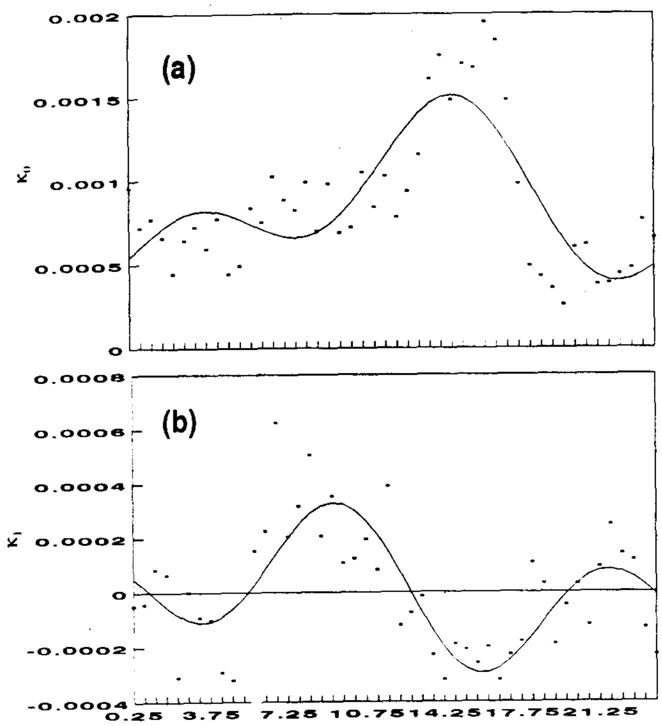

Fig. 6. Variables κ_0 (a) and κ_1 (b) estimated from equation (4) (see text) fit with a three-term Fourier series; estimated coefficients are presented in Table 1.

Because κ_2 values estimated from equation (4) appear to be stationary over time, the mean (115.2) was used to produce the final *SLOPE* estimates. Re-estimated values of σ_0 and κ_1 had harmonic changing patterns so that we used a three-term Fourier series in the second-stage non-linear regression of the form:

$$\kappa_0, \kappa_1 = A_0 + A_1 \sin[\pi(t+\omega_1)/12] + A_2 \cos[\pi(t+\omega_2)]$$

$$\text{MSE} = 7.413 \times 10^{-8} \quad \text{for } \kappa_0$$

$$\text{MSE} = 2.182 \times 10^{-8} \quad \text{for } \kappa_1$$

where A_0 is the mean value A_1 and A_2 are the amplitudes of the first and second harmonics of the series, and ω_1 and ω_2 are the phase changes. The predicted patterns of κ_0 and κ_1 are illustrated in Fig. 6 and estimated coefficients listed in Table 1.

Because the variable y has a discontinuity at 14:40 h (Fig. 7), a linear smoothing technique (Harvey, 1981) was used over the 3-h window 12.90–15.90 to make a smooth prediction and still minimize the residuals.

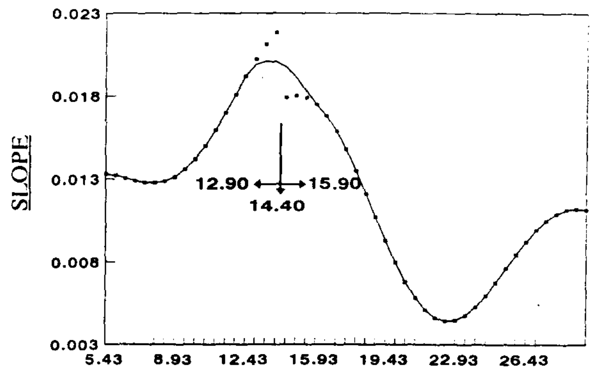

Fig. 7. Linear smoothing of discontinuity feature resulting from estimating the changing ratio of diurnal air temperatures from edge into interior (*SLOPE*) in second-stage regression with different independent variables for the periods before and after 14.40 h, the computed mean time of maximum temperature.

MODEL EVALUATION

The diurnal air-temperature gradients from the edge into interior forest simulated by the model are similar to those described by Chen (1991). Air temperature varied sinusoidally over the simulation period (Fig. 8), increasing exponentially during the day and decreasing at night with distance from the edge. In the mid-morning and late afternoon, there was little to no difference in air temperature (horizontal line) at the edge and inside the forest. Figure 8 further illustrates the influence of local macroclimate on air temperature gradients; on warm, sunny days (Fig. 8a) the gradients are sharper and on cool, cloudy days weaker (Fig. 8b).

The influence of edge orientation is evident by comparing both simulated maximum air temperatures at four contrasting edges (0 m; Fig. 9) and

TABLE 1

Estimated coefficients for κ_0 and κ_1 in second-stage regression (equation 4) for determining *SLOPE* estimates

Parameter [a]	κ_0	κ_1
A_0	8.6905×10^{-5}	1.6946×10^{-6}
A_1	3.756×10^{-5}	1.5024×10^{-4}
A_2	2.8765×10^{-5}	2.0443×10^{-4}
ω_1	1.633×10	1.084×10
ω_2	8.91	-1.594×10

[a] A_0 = mean; A_1, A_2 = amplitudes of first and second harmonics; ω_1, ω_2 = phase changes.

estimating the changing
:) in second-stage regres-
e and after 14.40 h, the

e into interior forest
by Chen (1991). Air
riod (Fig. 8), increas-
it with distance from
ere was little to no
edge and inside the
al macroclimate on
a) the gradients are

nparing both simu-
es (0 m; Fig. 9) and

ition 4) for determining

<10⁻⁶

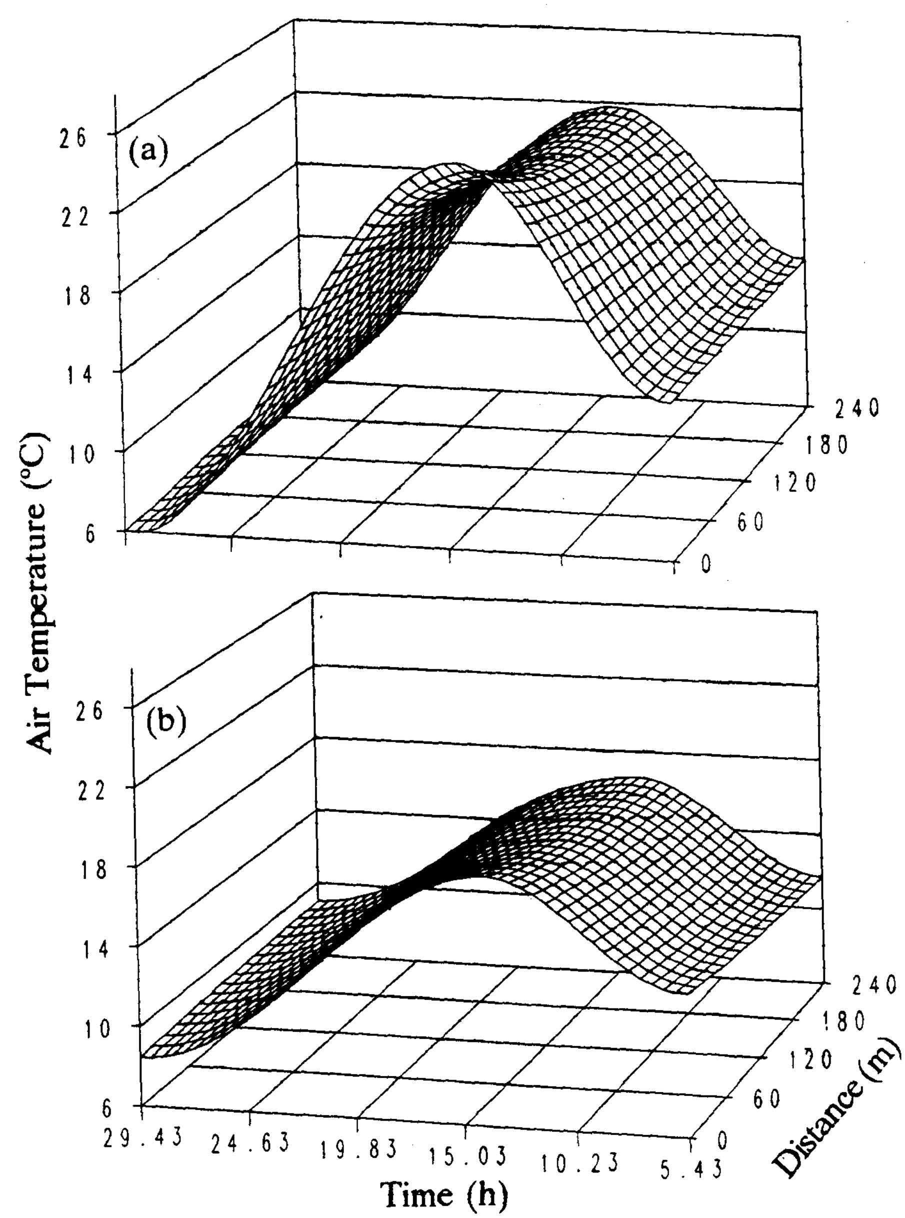

Fig. 8. Simulated diurnal air-temperature gradients with distance from the edge into interior forest as influenced by macroclimate: (a) for a warm, sunny day (7 September 1990), model inputs were $T_{max} = 24.63$, $T_{min} = 17.78$, $T_{max1} = 25.87$, $T_{min2} = 5.11$ (all °C), and $\theta = 225°$; (b) for a cool, cloudy day 23 August 1989, model inputs were $T_{max} = 17.56$, $T_{min} = 10.25$, $T_{max1} = 17.19$, $T_{min2} = 8.17$ (all °C), and $\theta = 45°$.

$<10^{-6}$
$<10^{-4}$
$<10^{-4}$
10
10

, ω_2 = phase changes.

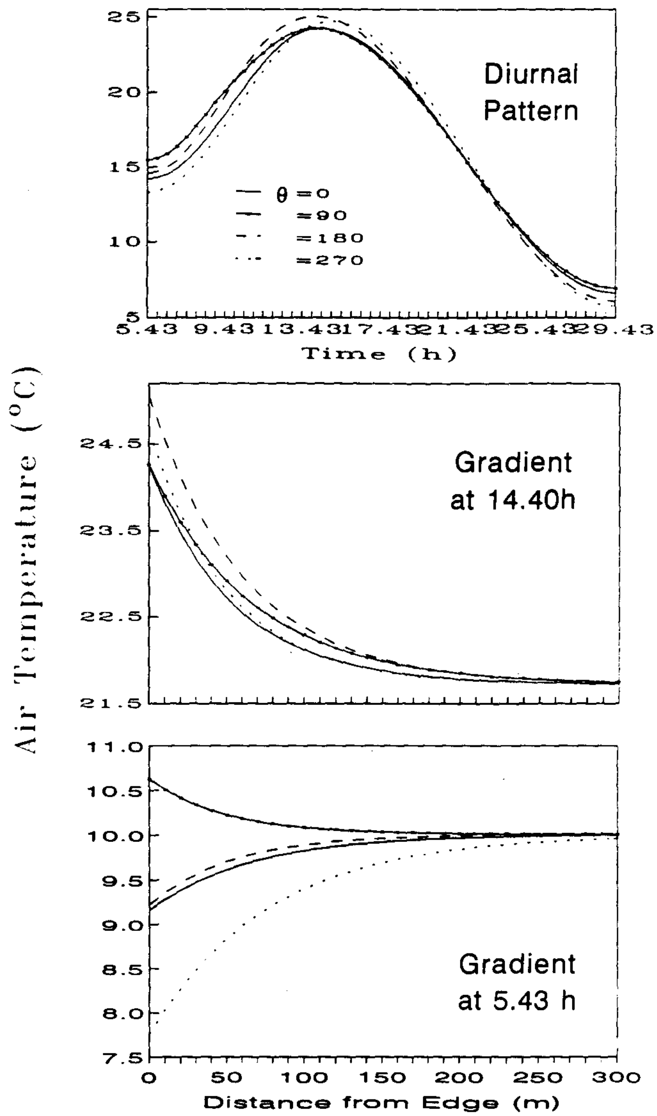

Fig. 9. Simulated maximum diurnal air-temperatures at four edges (0 m) as influenced by edge orientation (θ) and diurnal air-temperature gradients at four θs at the computed mean time of maximum (14.40 h) and minimum (5.43 h) temperatures for the following macroclimatic model inputs: $T_{max} = 26.0$, $T_{min} = 10.0$, $T_{max1} = 27.0$, $T_{min2} = 15.2$ (all °C).

air temperature gradients with distance from the edge for different edge orientations (Fig. 10). In the early morning, temperature is highest (11.8°C at 5.43 h) at an east-facing edge, which receives direct sunlight then, and lowest (9.4°C) at a west-facing edge, which is completely shaded (Fig. 9). However, temperature at an east-facing edge peaks earliest (13.93 h) of all

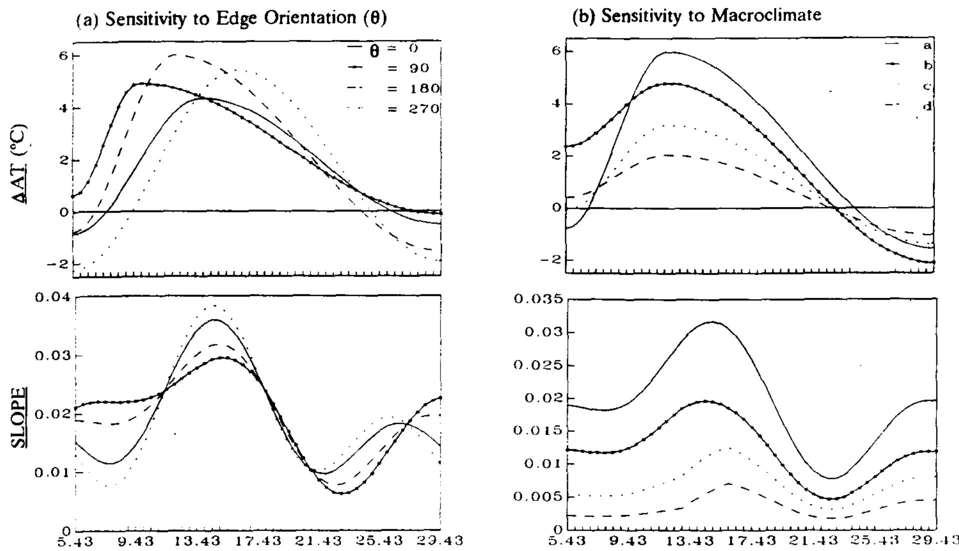

Fig. 10. Sensitivity of ΔAT and *SLOPE* (a) to edge orientation (θ) for the macroclimatic model inputs (15 July 1990) $T_{max} = 38.89$, $T_{min} = 9.13$, $T_{max1} = 26.9$, $T_{min2} = 9.41$ (all °C), and (b) at a south-facing edge ($\theta = 180°$) for the macroclimatic model inputs for the same day given in Table 2.

four edges and that at a west-facing edge latest (15.93 h). Air temperature at a south-facing edge lags about 2 h behind that at an east-facing edge but peaks highest of all four edges (14.43 h).

At 14.40 h, the computed mean time of maximum temperature in the simulation period, air temperatures decline with distance from the edge into interior forest, although south- and west-facing edges have steeper temperature gradients (temperature differences of 4.04 and 3.63°C, respectively) than do the other edge orientations (Fig. 10a). The depth of edge influence is greater at the east- and south-facing edges than at the other two orientations because east and south edges receive radiation earlier in the day than do the other two and have longer periods for edge effects to accumulate. However, at 5.43 h, the computed mean time of minimum temperature in the simulation period, temperatures decrease with distance from the edge at east-facing orientations, increase at west-facing orientations, and remain relatively unchanged at north- and south-facing orientations (Fig. 10b). These differences all relate to the distribution of solar radiation over time.

Generally, the combination of a larger ΔAT and a smaller *SLOPE* indicates a stronger and deeper edge effect, the combination of a smaller ΔAT and a larger *SLOPE* a weaker (or no) edge effect. Evaluation of edge effects becomes more complicated, however, with all other combinations of these two variables. For example, it is difficult to evaluate the significance of edge effects for air temperature gradients at east- and west-facing edges in the mid-afternoon (Fig. 10a), where both ΔAT and *SLOPE* are smaller; an index, such as degree days, has been frequently used in analyzing biological responses. Application of this index, however, is also questionable in analyzing many biological processes. Further study is urgently needed to understand how ΔAT and *SLOPE*, separately and in combination, characterize edge effects.

Sensitivity analysis showed that *TEMPIF*, computed independent of edge orientation, is indeed very sensitive to the input values for macroclimate. Recall from model development (see Fig. 1 and related text) that *TEMPIF* is linearly related to the maximum and minimum air temperatures in the clearcut; the equation coefficients (0.7556 and 0.8566, respectively) reflect the air-temperature differences in these two environments.

ΔAT and *SLOPE*, computed on the basis of edge orientation and macroclimate, were found to be sensitive to both, as determined by a test on an extremely hot day (15 July 1990). ΔAT was highest (0.62°C) at 5.43 h and peaked earliest (9.93 h) at an east-facing edge, which received direct solar radiation earliest; it peaked highest (5.98°C) at a south-facing edge, latest (15.93 h) at a west-facing edge, and at about the same time (13.93 h) at a north-facing edge as did maximum air temperature in the clearcut (Fig. 10a). *SLOPE* values at east- and south-facing edges were smaller than those at north- and west-facing edges (Fig. 10a), a smaller value indicating a greater depth of edge influence (recall Fig. 5). At night, values for both variables differed little among the four edge orientations. ΔAT and *SLOPE* values varied considerably according to macroclimate conditions (Fig. 10b, Table 2). When the weather was stable and cool (conditions c and d, Table

TABLE 2

Simulation inputs (°C) for four different weather conditions (a, b, c and d) and their daily temperature differences

Input [a]	a	b	c	d
T_{max}	38.89	24.84	19.88	17.19
T_{min}	9.13	6.15	11.13	13.15
T_{max1}	35.52	18.03	23.84	20.22
T_{min2}	9.41	7.27	7.99	10.25
Daily difference ($T_{max}-T_{min}$)	29.76	18.69	11.89	4.04

[a] T_{max} = daily maximum air temperature; T_{min} = daily minimum air temperature; T_{max1} = previous days' maximum air temperature; T_{min2} = next day's minimum air temperature.

2), ΔAT and *SLOPE* values are small, indicating a weak edge effect. With warmer and more variable weather (conditions a and b), values for ΔAT and *SLOPE* increased, and edge effects became stronger and more distinctive.

The model has two weaknesses. First, using sinusoidal curves may be problematical. These curves were divided in two, with the two sections joined to maintain least squares error (nonlinear regression) or averaged locally (i.e., for *SLOPE*). Sinusoidal functions were used throughout model development because both the first and second derivatives at the conjugations of the two sections of the curve were zero, indicating a smooth, continuous regression line there and a minimum error. However, with sinusoidal functions, the modeler has less control of the changing ratios of the dependent variables over time. A solution would be to use more Fourier terms, but this might create problems of overparameterization or further analysis of regression residuals. Nevertheless, other types of functions (e.g. exponential) should be explored for estimating the parameters involved in the regression analysis.

Second, the technique for estimating regression coefficients (parameters) is problematical. With this method, only the mean was computed, and the variances associated with the mean were not carried through model construction. Because of the large number of regressions (about 700 000), we did not check the error distributions but instead assumed a normal distribution with zero mean for residuals. However, further analysis of the variances may help increase model capability and improve precision so that the model might be applied more widely and help provide some other unusual cases.

Despite the preceding weaknesses, this empirical model successfully produced diurnal air-temperature gradients from the edge into interior forest, circumventing the need for time-consuming field measurements with expensive meteorological instruments and generating new information about the effects of edge orientation and macroclimate on air temperatures. Although applications of the model should be limited to recently created edges (i.e. 10- to 15-year-old clearcuts) adjacent to old-growth Douglas-fir forests on relatively flat (< 10°) terrain, our modeling approach could be applied to other types of edges by modifying the relationships developed herein for *TEMPIF*, ΔAT, and *SLOPE* with information about other variables (e.g., edge age, forest structure near the edge, seasonal dynamics of regional weather conditions, topographic features). We think that this model can be to be a powerful tool for evaluating edge effects in the forested landscape.

ACKNOWLEDGEMENT

The study was supported by a Prentice and Virginia Bloedel Professorship awarded to the College of Forest Resources, University of Washington; the Pacific Northwest Research Station, USDA Forest Service; and grants awarded to the Olympic Natural Resources Center by USDA Forest Service New Perspective's Program. We thank Carol Perry, Steve Lowe, and Douglas Maguire for review and helpful suggestions.

REFERENCES

Acock, B., Reddy, V.R., Whisler, F.D., Baker, D.N., McKinion, J.M., Hodges, H.F. and Boote, K.J., 1983. Response of vegetation to carbon dioxide 002. The soybean simulator GLYCIM: model documentation 1982. Joint program of the U.S. Department of Energy, Carbon Dioxide Research Division, and USDA Agricultural Research Service, conducted at USDA-ARS Crop Simulation Unit and Department of Agronomy, Mississippi Agricultural and Forest Experimental Station.

Allen, J.C., 1976. A modified sine wave method for calculating degree days. Environ. Entomol., 5: 388–396.

Beck, J.A. and Trevitt, A.C.F., 1989. Forecasting diurnal variations in meteorological parameters for predicting fire behavior. Can. J. For. Res., 19: 791–797.

Bocock, K.L., Jeffers, J.N.R., Lindley, D.K., Adamson, J.K. and Gill, C.A., 1977. Estimating woodland soil temperature from air temperature and other climatic variables. Agric. Meteorol., 18: 351–372.

Campbell, G.S., 1986. An Introduction to Environmental Biophysics. Springer-Verlag, New York, NY.

Carson, J.E., 1963. Analysis of soil and air temperatures by Fourier techniques. J. Geophys. Res., 68: 2217–2232.

Chapin III, F.S., Bloom, A.J., Field, C.B. and Waring, R.H., 1987. Plant responses to multiple environmental factors. BioScience, 37 (1): 49–57.

Chen, J., 1991. Edge effects: microclimate pattern and biological responses in old-growth Douglas-fir forests. Ph.D. Thesis, University of Washington, Seattle, WA.

Chen, J., Franklin, J.F. and Spies, T.A., 1992. Vegetation responses to edge environments in old-growth Douglas-fir forests. Ecol. Appl., 2 (4): 387–396.

Dale, V.H. and Hemstrom, M., 1984. CLIMACS: a computer model of forest stand development for western Oregon and Washington. USDA-FS Research Paper, PNW-327.

DeWit, C.T., Goudriaan, J. and VanLaar, H.H., 1978. Simulation of Simulation. Respiration and Transpiration of Crops. Pudoc, Wageningen, The Netherlands.

Dreistadt, S.H., Dahlsten, D.L., Rowney, D.L., Tait, S.M., Yokota, G.Y. and Copper, W.A., 1991. Treatment of destructive elm leaf beetle should be timed by temperature. Calif. Agric., March/April: 23–25.

Dwyer, L.M., Hayhoe, H.N. and Culley, J.L.B., 1990. Prediction of soil temperature from air temperature for estimating corn emergence. Agric. For. Meteorol., 70: 619–628.

Edmonds, R.L., 1987. Decomposition rates and nutrient dynamics in small-diameter woody litter in four forest ecosystems in Washington, U.S.A. Can. J. For. Res., 17: 499–509.

Floyd, R.B. and Braddock, R.D., 1984. A simple method for fitting average diurnal temperature curves. Agric. For. Meteorol., 32: 107–119.

ginia Bloedel Professor-
, University of Washing-
DA Forest Service; and
Center by USDA Forest
arol Perry, Steve Lowe,
stions.

ion, J.M., Hodges, H.F. and
e 002. The soybean simulator
U.S. Department of Energy,
ural Research Service, con-
ent of Agronomy, Mississippi

ating degree days. Environ.

variations in meteorological
9: 791–797.
Gill, C.A., 1977. Estimating
er climatic variables. Agric.

iysics. Springer-Verlag, New

rier techniques. J. Geophys.

, 1987. Plant responses to

cal responses in old-growth
Seattle, WA.
ses to edge environments in

er model of forest stand
Research Paper, PNW-327.
on of Simulation. Respira-
etherlands.
a, G.Y. and Copper, W.A.,
ied by temperature. Calif.

f soil temperature from air
orol., 70: 619–628.
s in small-diameter woody
For. Res., 17: 499–509.
r fitting average diurnal

Franklin, J.F., 1989. Toward a new forestry. Am. For. November/December: 37–44.

Franklin, J.F. and Dyrness, C.T., 1973. Natural vegetation of Oregon and Washington. USDA-FS Technical Report, PNW-8.

Franklin, J.F. and Forman, R.T.T., 1987. Creating landscape patterns by forest cutting: ecological consequences and principles. Landscape Ecol., 1: 5–18.

Franklin, J.F., Cromack, Jr., K., Denison, W., McKee, A., Maser, C., Sedell, J. Swanson, F. and Juday, G., 1981. Ecological characteristics of old-growth Douglas-fir forests. USDA-FS General Technical Report, PNW-118.

Harvey, A.C., 1981. Time Series Models. John Wiley & Sons, New York, NY.

Hoogenboom, G. and Huck, M.G., 1986. ROOTSIMU v. 40. A dynamic simulation of root growth, water uptake, and biomass partitioning in a soil–plant–atmosphere continuum: Update and documentation. Agronomy and Soils Dept. Series 109, Alabama Agricultural Exp. Station. 83 pp.

Hungerford, R.D., Nemani, R.R., Running, S.W. and Coughlan, J.C., 1989. MTCLIM: a mountain microclimate simulation model. USDA-FS Research Paper, INT-414.

Lee, R., 1978. Forest Microclimatology. Columbia University Press, New York. USA.

Lehmkuhl, J.F. and Ruggiero, L.F., 1991. Forest fragmentation in the pacific Northwest and its potential effects on wildlife. In: L.F. Ruggiero, K.B. Carey and M.H. Huff (tech. coords.), Wildlife and vegetation of unmanaged Douglas-fir forests. General Technical Report, PNW-GTR-285, USDA, Forest Service, pp. 35–46.

Lemon, E. Steward, D.W. and Shawcraft, R.W., 1971. The sun's works in a cornfield. Science, 174: 371–378.

Miller, D.R., 1980. The two-dimensional energy budget of a forest edge with field measurements at a forest-parking lot interface. Agric. Meteorol., 22: 53–78.

Myrup, L.O., 1969. A numerical model of the urban heat island. J. Appl. Meteorol., 8: 908–918.

Parton, W.J. and Logan, J.A., 1981. A model for diurnal variation in soil and air temperature. Agric. Meteorol., 23: 205–216.

Peters, R.L., 1990. Effects of global warming on forests. For. Ecol. Manage., 35: 13–33.

Reicosky, D.C., Winkelman, L.J., Baker, J.M. and Baker, D.G., 1989. Accuracy of hourly air temperatures calculated from daily minima and maxima. Agric. For. Meteorol., 46: 193–209.

Rothermel, R.C., Wilson, Jr., R.A., Morris, G.A. and Sacket, S.S., 1986. Modeling moisture content of fine dead wildland fuels: input to the BEHAVE fire prediction system. USDA-FS Note, INT-359.

Running, S.W., Nemani, R.R., Peterson, D.L., Band, L.E., Potts, D.F., Pierce, L.L. and Spanner, M.A., 1989. Mapping regional forest evapotranspiration and photosynthesis by coupling satellite data with ecosystem simulation. Ecology, 70: 1090–1101.

Taconet, O., Bernard, R. and Vidal-Majar, D., 1986. Evapotranspiration over an agricultural region using a surface flux/temperature model based on NOAA-AVHRR data. Climate Appl. Meteorol., 25: 284–307.

Walter, A., 1967. Notes on the utilization of records from third order climatological stations for agricultural purposes. Agric. Meteorol., 4: 137–143.

Wann, M., Yen, D. and Gold, H.J., 1985. Evaluation and calibration of three models for daily cycle of air temperature. Agric. For. Meteorol., 34: 121–128.

Waring, R.H. and Franklin, J.F., 1979. Evergreen coniferous forests of the Pacific Northwest. Science, 204: 1380–1386.

Watanabe, N., 1978. An improved method for calculating heat accumulation from daily maximum and minimum temperatures. Appl. Entomol. Zool., 13: 44–46.

Yahner, R.H., 1988. Changes in wildlife communities near edges. Conserv. Biol., 2(4): 333–339.

Zobel, D.B., Mckee, A., Hawk, G.M. and Dyrness, C.T., 1976. Relationships of environment to composition, structure, and diversity of forest communities of the central western Cascades of Oregon. Ecol. Monogr., 46 (2): 135–156.